Radio Interferometric Studies of Cool Evolved Stellar Winds

A dissertation submitted to the University of Dublin
for the degree of Doctor of Philosophy

Eamon O'Gorman

Supervisor: Dr. Graham M. Harper

Trinity College Dublin, September 2013

School of Physics
University of Dublin
Trinity College

Declaration

I declare that this thesis has not been submitted as an exercise for a degree at this or any other university and it is entirely my own work.

I agree to deposit this thesis in the University's open access institutional repository or allow the library to do so on my behalf, subject to Irish Copyright Legislation and Trinity College Library conditions of use and acknowledgement.

Name: Your Name

Signature: .... **Date:** ....

Summary

You should write a nice summary here...

A dedication if you wish...

Acknowledgements

Some sincere acknowledgements...

List of Publications

Refereed

1. **O'Gorman, E.**, Harper, G. M., Brown, A., Brown, A., Drake, S., and Richards, A. M. S.
   "Multi-wavelength Radio Continuum Emission Studies of Dust-free Red Giants"
   The Astronomical Journal, *In press*, (2013)

2. Richards, A. M. S., Davis, R. J., Decin, L., Etoka, S., Harper, G. M., Lim, J. J., Garrington, S. T., Gray, M. D., McDonald, I., **O'Gorman, E.**, Wittkowski, M.
   "e-MERLIN resolves Betelgeuse at wavelength 5 cm"
   Monthly Notices of the Royal Astronomical Society Letters, 432, L61 (2013)

3. **O'Gorman, E.**, Harper, G. M., Brown, J. M., Brown, A., Redfield, S., Richter, M. J., and Requena-Torres, M. A.
   "CARMA CO(J = 2 - 1) Observations of the Circumstellar Envelope of Betelgeuse"
   The Astronomical Journal, 144, 36 (2012)

4. Sada, P. V., Deming, D., Jennings, D. E., Jackson, B. K., Hamilton, C. M., Fraine, J., Peterson, S. W., Haase, F., Bays, K., Lunsford, A., and **O'Gorman, E.**
   "Extrasolar Planet Transits Observed at Kitt Peak National Observatory"
   Publications of the Astronomical Society of the Pacific, 124, 212 (2012)

5. Sada, P. V., Deming, D., Jackson, B. K., Jennings, D. E., Peterson, S. W., Haase, F., Bays, K., **O'Gorman, E.**, and Lundsford, A.
   "Recent Transits of the Super-Earth Exoplanet GJ 1214b"
   The Astrophysical Journal Letters, 720, L215 (2010)

Non-Refereed

1. **O'Gorman, E.**, & Harper, G. M.
   "What is Heating Arcturus' Wind?",
   Proceedings of the 16th Cambridge Workshop on Cool Stars, Stellar Systems and the Sun. Astronomical Society of the Pacific Conference Series, 448, 691 (2011)

Contents

List of Figures

List of Tables

1

A Thermal Energy Balance for Arcturus' Outflow

The chapter investigates the various heating and cooling processes that control the thermal structure of Arcturus' mass outflow region. We use the hybrid chromosphere and wind model derived in Section **??** as the basis to derive the magnitude of these processes as function of distance from the star. The effect of adiabatic expansion cooling and cooling by various lines are investigated. This work is a continuation of the initial findings of O'Gorman & Harper (2011).

1.1 Motivation for a Thermal Energy Balance

We have shown in Chapter **??** that for a monotonic ideal gas, the energy per unit mass, $u(r)$, is the sum of the kinetic and gravitational energies, and the enthalpy

$$u(r) = \frac{v(r)^2}{2} - \frac{GM_\star}{r} + \frac{5\mathfrak{R}T}{2\mu}. \tag{1.1}$$

The lower boundary of a stellar outflow is the photosphere which is gravitationally bound to the star. This implies that the energy in Equation 1.1 must be negative at this point. If a star is to have an outflow, then its energy must become positive at large r to escape the gravitational well [i.e., $v(r)^2 \geq v_{\rm esc}(r)^2$]. Therefore, energy must be added to the gas if its velocity is to reach (or exceed) the local escape velocity. The addition of this energy can be either in the form of heat input per unit mass, $q(r)$, or in the form of momentum input [i.e., an outward force, $f(r)$]. In other words, differentiating Equation 1.1 with respect to r gives the change in energy per distance from the star, and this becomes

$$\frac{d\,u(r)}{dr} = f(r) + q(r), \tag{1.2}$$

which is just a form of the *Bernoulli* equation. The unknown fundamental mechanisms responsible for driving the winds of cool evolved stars must therefore manifest themselves in either one or both of the quantities on the right hand side of Equation 1.2. Therefore, studying the heating deposition , $q(r)$, taking place in Arcturus's outflow is a valuable exercise and should provide insight into its wind driving mechanism(s).

Our multi-wavelength radio study of Arcturus allowed us to refine its existing atmospheric model. We found that our long wavelength VLA flux density measurements could be reproduced by the existing model if the almost isothermal outflow was replaced with an outflow that contained a large thermal gradient. This new hybrid model is graphically summarized in Figure **??**. The goal in this chapter is to use this new model as a foundation to study the thermal energy balance in Arcturus's atmosphere. The simple idea behind this is that all the heating and cooling processes taking place in the outflow should combine to produce the derived thermal profile from Chapter ??. Knowing the main mechanisms through which the plasma can cool thus allows us to examine the possible mechanisms which heat the plasma to the known temperature. Investigating the magnitude of the heating deposition of various mechanisms then then tells us if such a mechanism can play a part in the mass loss process.

1.2 Thermal Model for a Spherically Symmetric Outflow

In this section we derive an expression to describe how the temperature in a stellar outflow changes as a function of distance from the star. In doing so, we also present the notation that is used in subsequent sections to describe the magnitude of the heating and cooling taking place at certain regions in a stellar outflow. We assume all quantities vary radially (i.e, spherical symmetry) and that the mass loss rate is constant (i.e., time independent). The continuity equation can then be written as

$$v\frac{d\rho}{dr} = -\rho\left(\frac{dv}{dr} + \frac{2v}{r}\right) \tag{1.3}$$

where v and ρ are the flow velocity and mass density at a distance r from the star. The first law of thermodynamics tells us that the change in internal energy of a system is equal to the heat added to the system minus the work done by the system on its environment. For a reversible process in a closed system the work done is PdV, where P and V are the pressure and volume of the system. Writing the first law of thermodynamics in terms of rates per unit mass then gives

$$\frac{du}{dt} = \frac{dq}{dt} - \frac{P}{m}\frac{dV}{dt} \tag{1.4}$$

where u is the internal energy per unit mass and q is the net heat gained per unit mass. The time dependence in the first and last terms can be switched to a radial dependence via $v = dr/dt$, and m/ρ can be substituted for V to get

$$v\frac{du}{dr} = -\frac{P}{\rho}\left(v\frac{d\rho}{dr}\right) + \frac{dq}{dt}. \tag{1.5}$$

Substituting in Equation 1.3 and using $u = 3nkT/2\rho$ and $P = nkT$ gives

$$v\left(\frac{3nk}{2\rho}\frac{dT}{dr}\right) = -\frac{nkT}{\rho}\left(\frac{dv}{dr} + \frac{2v}{r}\right) + \frac{dq}{dt}. \tag{1.6}$$

If we define Γ and Λ are the heating and cooling rates per unit volume respectively, then we can rearrange this equation to get

$$\frac{dT}{dr} = -\frac{4T}{3r} - \frac{2T}{3v}\frac{dv}{dr} + \frac{2(\Gamma - \Lambda)}{3nkv}. \tag{1.7}$$

The first two terms on the right account for adiabatic expansion cooling. The second term is important in the wind acceleration region but is zero once the wind has reached its terminal velocity. The third term accounts for all other heating and cooling processes. This equation is equivalent to Equation 8 in Goldreich & Scoville (1976) and can also be written in dimensionless form (Rodgers & Glassgold, 1991) by multiplying across by r/T as follows:

$$\frac{d(\ln T)}{d(\ln r)} = -\frac{4}{3} - \frac{2}{3}\frac{d(\ln v)}{d(\ln r)} + \sum_{i=1}\mathcal{H}_i - \sum_{j=1}\mathcal{L}_j \tag{1.8}$$

where

$$\mathcal{H}_i = \frac{2r}{3nkvT}\Gamma_i \tag{1.9}$$

and

$$\mathcal{L}_j = \frac{2r}{3nkvT}\Lambda_j \tag{1.10}$$

are the various heating and cooling contributions respectively, normalized to constant velocity adiabatic expansion cooling. Finally this equation can be expressed in terms of the gas kinetic temperature's local power law slope, λ,

$$\frac{d(\ln T)}{d(\ln r)} = -\lambda \tag{1.11}$$

where

$$\lambda = \lambda_0 + \sum_{i=1}\lambda_i \tag{1.12}$$

which contains all of the wind heating and cooling processes, including that from adiabatic expansion cooling, λ_0. We note that positive and negative λ's represent cooling and heating, respectively. This notation will be used throughout this chapter and allows the various heating and cooling process to be easily compared to the 4/3 exponent, characteristic of a constant velocity outflow undergoing adiabatic expansion cooling.

1.3 Cooling Processes

The three ways in which the gas in Arcturus' partially ionized outflow can cool are through adiabatic expansion, radiative recombination, and collisional excitation of neutral and ionized atoms. We now assess the importance of each of these cooling processes between $\sim 1 - 10\,R_\star$.

1.3.1 Adiabatic Expansion Cooling

Adiabatic expansion cooling is the thermodynamic process in which a fixed quantity of gas cools as it expands into a larger volume of gas. It is composed of a geometric term and a velocity gradient term; these being the first two terms on the right of Equation 1.8. As shown in Figure 1.1, the dominant term close to the photosphere is the velocity gradient term due to the rapid wind acceleration while further out where the wind reaches its terminal velocity, the geometric term becomes dominant. Adiabatic expansion cooling is a very efficient cooling mechanism in the atmospheres of all stars. To show this we take the atmosphere of Arcturus as an example and assume the absence of all heating mechanisms. The geometric factor alone then will lower the gas temperature to decrease by a factor of 10^4 by $1500\,R_\star$ which is below the cosmic background temperature.

1.3.2 Radiative Recombination Cooling

Radiative recombination is the process by which an electron is captured by an ion into a bound state n with the emission of a photon. The overwhelming abundance of H along with it having a similar cross section for capture to heavier ions, means that it is by far the most important species to consider for this cooling process. The radiative recombination cooling rate is

$$\Lambda = n_{HII} n_e \alpha^n \left(\frac{3}{2}kT\right) \qquad \mathrm{erg\,s^{-1}\,cm^{-3}} \tag{1.13}$$

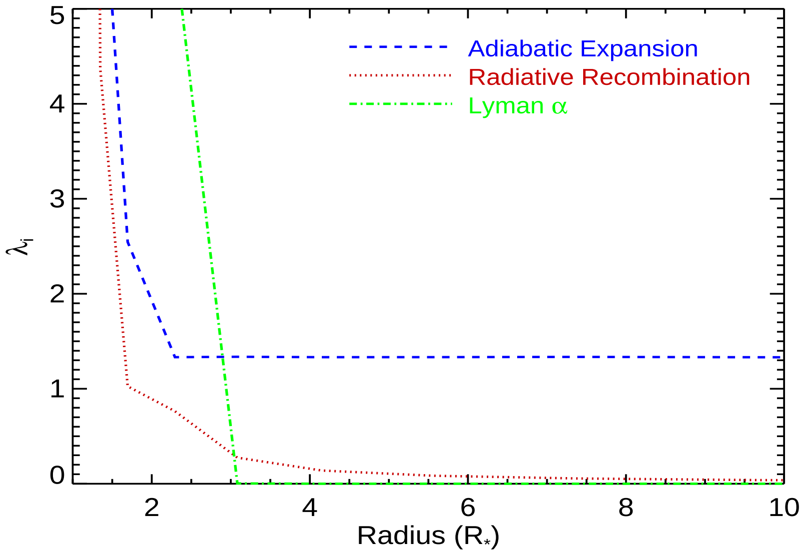

Figure 1.1: The net cooling from adiabatic expansion, radiative recombination, and Lyman α cooling in Arcturus' outflow. For adiabatic expansion cooling, the dominant term close to the photosphere is the velocity gradient term from Equation 1.8 due to the rapid wind acceleration, while further out where the wind reaches its terminal velocity, the geometric term becomes dominant. Radiative recombination is also an important cooling mechanism between $\sim 1-4\,R_{\star}$. The Lyman α cooling function is very sensitive to T and is the dominant cooling process out to $2.8\,R_{\star}$.

where $\frac{3}{2}kT$ is the average thermal energy of a captured electron and α^n is the hydrogen recombination rate coefficient summed over n levels. The hydrogen recombination rate coefficient excluding captures to the $n = 1$ level is given as

$$\alpha_B = \frac{2.06 \times 10^{-11}}{T^{1/2}} \phi_2(\beta) \qquad \mathrm{s^{-1}\,cm^3}. \tag{1.14}$$

$\phi_2(\beta)$ is a function that varies with temperature and has been tabulated for various temperatures by (Spitzer, 1978). Recombination to the ground state is excluded because the process produces another ionizing photon that can be easily absorbed again, producing the net effect that the recombination had not occurred. The radiative recombination cooling contribution can then be calculated using Equation 1.10.

1.3.3 Lyman-alpha Cooling

Collisions between electrons and gas atoms (or ions) causes energy to be exchanged between the thermal kinetic of the gas and the internal energy of the individual gas atoms (or ions). Collisional excitation cools the gas while collisional de-excitation heats the gas. At temperatures of a few thousand degrees, the excited levels in neural H can become populated from electron collisions and thus can be a source of cooling. The analytical expression for the resulting net cooling rate per volume is

$$\Lambda_{\rm eH} = 7.3 \times 10^{-19} n_{\rm e} n_{\rm HI} e^{-118{,}400/T(K)} \qquad {\rm erg\,s^{-1}\,cm^{-3}} \tag{1.15}$$

Spitzer (1978). Most of the resulting radiation comes from the $n = 2$ level (Lyman α) and this is why the cooling rate is almost proportional to $\exp(-E_{12}/kT)$, where $E_{12}/k = 118319\,K$. Equation 1.15 is a very sensitive function of the gas temperature and as can be seen from Figure 1.1, is the dominant cooling process out to $2.8\,R_\star$. The sharp falloff in temperature in Arcturus' outflow post $2.3\,R_\star$ results in this mechanism going from being a very efficient cooling process within $2.3\,R_\star$ to having a negligible effect by $\sim 3.1\,R_\star$.

1.3.4 Other Line Coolants

Due to its large abundance, H is expected to be the most efficient line cooling mechanism in the inner atmosphere of Arcturus. Nevertheless, it is also worth investigating the effects of line cooling from heavier elements which may become important at lower temperature further out in the atmosphere where line cooling from H has almost ceased. Line cooling from these heavy elements is due mainly to electron impact excitation of electronic levels of the neutral and ionized species at high temperatures, while at lower temperatures (i.e. further out in the CSE) line cooling is mainly due to the electron impact excitation of fine structure levels of the neutral and ionized constituents (Dalgarno & McCray, 1972). Table 1.1 lists the most relevant heavy elements for this study based on abundance and suitable line transitions. All heavy elements with an ionization potential (IP) lower than O were assumed fully ionized, while the ionization balance of O was based on the IUE line profile analysis of Judge (1986).

Table 1.1: Elemental Abundance in Arcturus's Outflow

Element	Abundance	IP (eV)	Reference
O	4.7×10^{-4}	13.6	Ramírez & Allende Prieto (2011)
C	2.1×10^{-4}	11.3	Ramírez & Allende Prieto (2011)
N[1]	6.7×10^{-5}	14.5	Asplund *et al.* (2009)
Mg	3.0×10^{-5}	7.6	Ramírez & Allende Prieto (2011)
Si	2.0×10^{-5}	8.2	Ramírez & Allende Prieto (2011)
Fe	1.0×10^{-5}	7.9	Decin *et al.* (2003)

[1] Assumed solar abundance.

The line cooling rate per unit volume due to the transition ul in a medium where the optical depth is not negligible is

$$\Lambda_{\text{line}} = \sum_{u \to l} n_u A_{ul} E_{ul} \rho(\tau) \qquad \mathrm{erg\,s^{-1}\,cm^{-3}} \tag{1.16}$$

where n_u is the population of the upper level, A_{ul} is the spontaneous emission coefficient of the transition, and E_{ul} is the energy of the radiated photon. Here, the sum is over all possible upper to lower transitions and $\rho(\tau)$ is the probability the photon will escape the gas without being reabsorbed. This function lowers the line cooling rate and can be written as

$$\rho(\tau) = \frac{1 - \exp(-3\tau/2)}{3\tau/2} \tag{1.17}$$

(Castor, 2004). The level populations were found by simultaneously solving the statistical equilibrium equations and the non-LTE fractional fractional populations formula, i.e.,

$$\frac{n_u}{n_l} = \frac{g_u}{g_l} \exp\left(\frac{-E_{21}}{kT}\right) \left(1 + \frac{n_{\text{cr}}}{n_{\text{tot}}}\right)^{-1}. \tag{1.18}$$

Here g_u and g_l are the degeneracy (the number of states with the same energy) of the levels and n_{tot} is the total number density of all particles in the gas. The critical density, n_{cr}, is the ratio of the radiative and collisional de-excitation rates

$$n_{\text{cr}} = \frac{A_{ul} \rho_{ul}}{C_{ul}}. \tag{1.19}$$

and tells us whether LTE is an accurate approximation at that point in the outflow.

The line cooling from these heavy elements was found to be only significant within $1.5\,R_\star$; the most efficient of which being the C II $^2P \rightarrow ^2P$ semi-forbidden transition (2326 Å). As the density decreases so too do the number of collisions, and so when atoms/ions radiate they are less likely to be re-excited. Therefore line cooling from these heavy elements is only important at high densities, i.e., close to the star. Line cooling due to the fine structure levels of these elements was found to be negligible due to the high temperature regime. In Figure 1.2 we plot the sum of all the cooling mechanisms taking place in Arcturus' outflow. The cooling taking place within the first $3\,R_\star$ is mainly due to Lyman Alpha emission line while the cooling further out is mainly due to gas expansion, with a small contribution from radiative recombination.

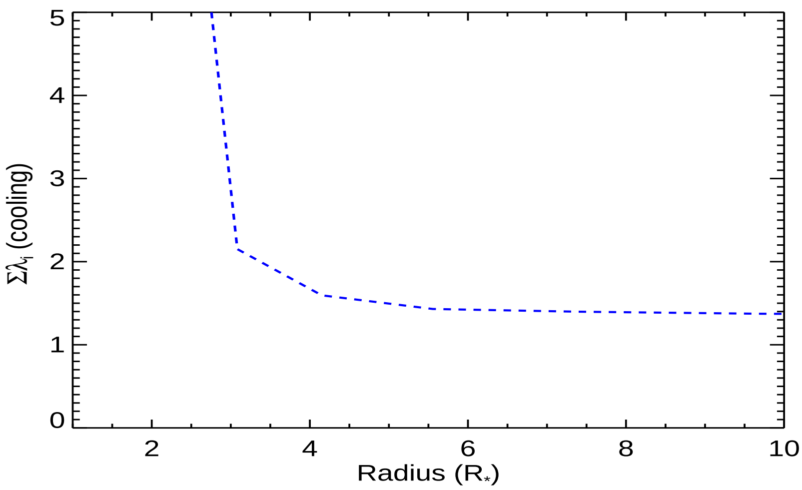

Figure 1.2: Summation of all the cooling mechanisms normalized to constant adiabatic cooling taking place in Arcturus' outflow. The cooling taking place within the first $3\,R\star$ is mainly due to Lyman Alpha emission line while the cooling further out is from gas expansion, with a small contribution from radiative recombination.

1.4 Heating Mechanisms

In the following sections we investigate various possible heating mechanisms taking place in Arcturus's outflow and the overall efficiency of these mechanisms at various distances from the star.

1.4.1 Photoionization Heating

The UV radiation field of Arcturus can photoionize atoms producing energetic electrons which heat the atmosphere. The energy released per second per unit volume due to the photoionization of an atom X can be written as

$$\Gamma(X) = n(X) \int_{\lambda_{min}}^{\lambda_{th}} \frac{4\pi J_\lambda}{E_\lambda} \sigma_X(\lambda)(E_\lambda - E_{\lambda_{th}}) d\lambda \tag{1.20}$$

Here, $E_\lambda - E_{\lambda_{th}}$ is the energy added to the gas by one ionization, i.e., the energy of the incident photon minus the threshold energy for ionization, which is specific to each element. J_λ is the mean intensity of radiation at a point and so $4\pi J_\lambda/E_\lambda$ is the number of incident photons per unit area per unit time per unit wavelength interval. $\sigma_X(\lambda)$ is the ionization cross section for an atom X by photons with an energy E_λ below a threshold wavelength, λ_{th}, and is a function of wavelength.

To calculate the mean intensity, the incident flux must be known. The flux at the stellar surface, $F_\star$, is related to the flux observed at Earth, $F_\oplus$, by

$$F_\star = \left(\frac{d}{R_\star}\right)^2 F_\oplus = \left(\frac{2}{\phi}\right)^2 F_\oplus \tag{1.21}$$

The mean intensity at a point in the atmosphere is then

$$J(r) = W(r) I_\star = \frac{W}{\pi} \left(\frac{2}{\phi}\right)^2 F_\oplus \tag{1.22}$$

where $W(r)$ is the radiation dilution factor and is given by

$$W(r) = \frac{1}{2}\left(1 - \sqrt{1 - \left(\frac{R_\star}{r}\right)^2}\right) \tag{1.23}$$

The incident flux measurements (i.e., $F_\oplus$) which vary as a function of wavelength were obtained from the online StarCAT catalog (Ayres, 2010). Any missing data was interpolated or extrapolated upon to provide a continuous $J(r)$ between 912 Åand 3646 Å [i.e., the ionization threshold for the H ($n = 2$) level]. The photoionization cross section values for atoms with IPs less than 13.6 eV along with the values for the H ($n = 2$) level were taken from Mathisen (1984) and are shown as a function of wavelength in Figure 1.3. The net heating due to photoionization was then found by using Equation 1.20 for each of these species resulting in significant heating inside $\sim 1.4\,R_\star$ as shown in Figure **??**. However, by $\sim 2\,R_\star$ its heating ability is about one order of magnitude weaker than adiabatic cooling at the same distance and so photoionization heating is not an efficient mechanism at heating Arcturus' outflow.

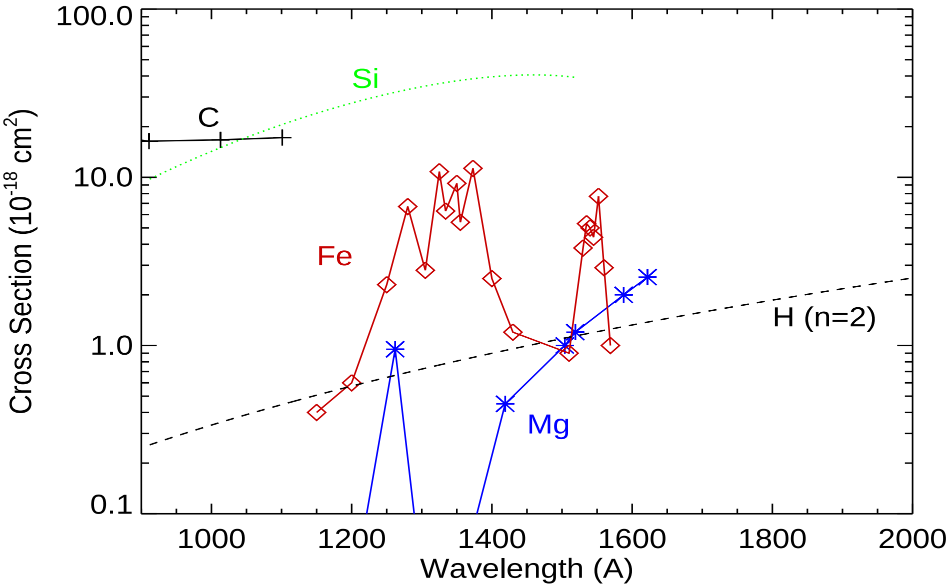

Figure 1.3: The photoionization cross section values for atoms with IPs less than 13.6 eV which were used in this study. The photoionization of H from the $n = 2$ level was also considered and its cross section is also shown. The ionization threshold for H (n=2) is 3646 Å.

1.4.2 Ambipolar Diffusion Heating

If a magnetic field remains frozen to the electrons and ions in a plasma, the charged plasma and field can drift through the gas of neutral atoms. The collisions, chiefly between positive ions and neutral hydrogen atoms (Spitzer, 1978), result in an exchange of momentum between the magnetic field and the neutral gas which results in a net heating. The recent possible detection of a weak ($B < 1\,G$) mean longitudinal magnetic field for Arcturus (Sennhauser & Berdyugina, 2011) suggests that ambipolar diffusion heating should be considered as a possible heating mechanism. We use the expression given by Shang *et al.* (2002) to define the volumetric rate of ambipolar diffusion

$$\Gamma = \frac{\rho_n |\mathbf{f}_L|^2}{\gamma \rho_i (\rho_n + \rho_i)^2}. \tag{1.24}$$

Here, ρ_n and ρ_i are the mass densities of the neutral and ionic species, respectively, γ is the ion-neutral momentum transfer coefficient, and $\mathbf{f}_L$ is the volumetric Lorentz force

$$\mathbf{f}_L = \frac{1}{4\pi}(\nabla \times \mathbf{B}) \times \mathbf{B}. \tag{1.25}$$

In Appendix **??** we give a derivation for Equation 1.24 and demonstrate how the γ coefficient can be transformed into a quartic equation by eliminating a term known as the slip velocity, w ($w \equiv v_i - v_n$). The derivation of 1.24 assumes that the difference in acceleration in the neutrals and ions can be ignored. As shown in Appendix **??**, the radial Lorentz force is found from the equation of motion:

$$\rho_n v_n \frac{dv_n}{dr} + \rho_i v_i \frac{dv_i}{dr} = -\frac{GM_\star}{r^2}(\rho_n + \rho_i) + \mathbf{f}_L. \tag{1.26}$$

This then allows the γ coefficient and thus the volumetric heating to be calculated. The effect of radial ambipolar diffusion heating was found to be about three orders of magnitude less than adiabatic constant velocity expansion cooling and is therefore a negligible heating mechanism. This is due to the relatively high ionization balance in Arcturus' outflow.

1.4.3 Turbulent Heating

The dissipation of turbulent fluctuations can make a significant contribution to the thermodynamic heating of a plasma, and has regularly been studied as a heating source of the solar corona and driving solar wind acceleration (e.g., Cranmer *et al.*, 2007; Lehe *et al.*, 2009). It has also been studied as a source of energy and momentum for accelerating cool evolved stellar winds (e.g., Falceta-Gonçalves *et al.*, 2006; Hartmann & MacGregor, 1980). These studies have focused on the dissipation of turbulent fluctuations from Magnetohydrodynamic (MHD) waves and we likewise make the same assumption. However, our simple phenomenological description of turbulent heating can also be explained by the dissipation of acoustic waves in an unmagnetized medium (e.g., Lighthill, 1952; Stein, 1967).

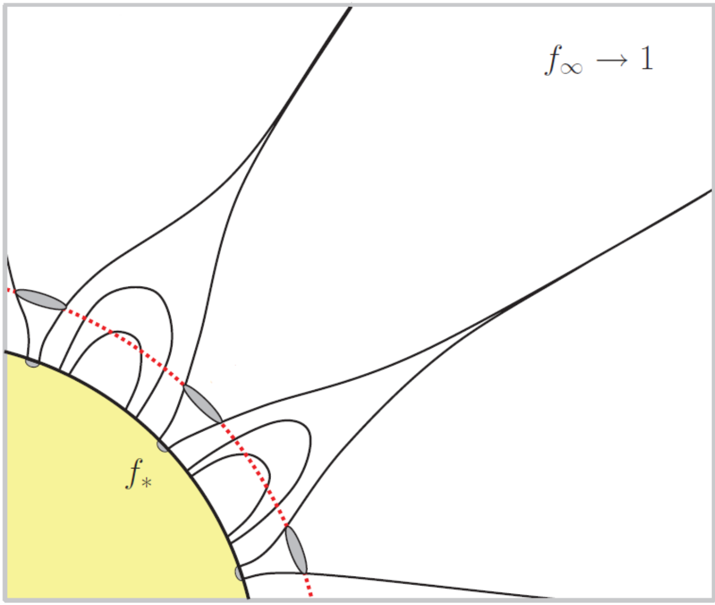

Figure 1.4: Example of diverging flux tubes in the atmosphere of a cool evolved star. The filling factor, f, of the open magnetic flux tubes grows from $f_\star \ll 1$ at the photosphere to an asymptotic value of $f_\infty \to 1$ at large distances. Alfvén waves then propagate up these flux tubes and are partially reflected, resulting in an interaction causing turbulence which dissipates into heating. Image adopted from Cranmer & Saar (2011).

The idea of MHD turbulent heating of Arcturus' atmosphere is based on what is known to happen in the solar atmosphere. For the Sun, most of the photospheric magnetic field is located in small flux tubes (of diameter $\sim 100\,\mathrm{km}$) concentrated in the intergranular downflow lanes with field strengths of $\sim 1400\,\mathrm{G}$ (Berger & Title, 2001). These flux tubes, whose geometries are shown in Figure 1.4, have relatively small photospheric filling factors of $f_\star \sim 0.1 - 1\,\%$, however, and so the total magnetic flux density is much lower when spatially averaged over the entire solar disk and is the order of $f_\star B_\star = 1 - 10\,\mathrm{G}$ (Schrijver & Harvey, 1989). The same structures may be present in the atmosphere of Arcturus, which possibly has a total magnetic flux of $f_\star B_\star \sim 0.5\,\mathrm{G}$ (Sennhauser & Berdyugina, 2011). Alfvén waves then propagate up these flux tubes and are partially reflected by radial gradients in the density and magnetic field strength. The counter-propagating wave packets then interact with one another along these flux tubes, developing into strong MHD turbulence (Iroshnikov, 1964). The energy flux in the cascade from large to small eddies terminates in dissipation and heating (e.g., Cranmer & van Ballegooijen, 2005; Matthaeus *et al.*, 1999)

In this study, we adopt the following phenomenological form for the MHD turbulent heating rate per unit volume,

$$\Gamma_{turb} = \frac{1}{2}\frac{\rho U^2}{L/U} \quad \mathrm{erg\ s^{-1}\ cm^{-3}} \tag{1.27}$$

where n_H is the number of hydrogen atoms, Σ is the mean mass per hydrogen nuclei, m_H is the mass of a hydrogen atom, U is the characteristic velocity and L is the characteristic length scale. The characteristic velocity is taken to be the local hydrogen sound speed and the characteristic length scale is the local density scale height. The subsequent heating contribution from this process can then be written as

$$\lambda_{turb} \propto \frac{m_H\sqrt{T}}{v}\frac{d(ln\ \rho)}{d(ln\ r)} \tag{1.28}$$

where v is the wind velocity.

This phenomenological description of turbulent heating has successfully reproduced many properties of coronal heating for the Sun (Cranmer, 2012).

Some descriptions of turbulence and magnetic reconnection specify only the energy that is input into the system on the largest spatial scales. These models thus employ various phenomenological assumptions about how that energy is eventually dissipated

and assumes an ideal kolmogorov (1941) hydrodynamic cascade see appendix l is the length of the largest driving eddies

A

List of Abbreviations Used in this Thesis.

Table A.1: List of Abbreviations

First entry	**Second entry**
BIMA	Berkeley Illinois Maryland Association
CARMA	Combined Array for Research in Millimeter-wave Astronomy
CSE	Circumstellar Envelope
DDT	Director's Discretionary Time
e-MERLIN	e-Multi-Element Radio Linked Interferometer Network
FOV	Field of View
GREAT	German Receiver for Astronomy at Terahertz Frequencies
HPBW	Half Power Beamwidth
HST	Hubble Space Telescope
IOTA	Infrared Optical Telescope Array
IR	Infrared
IRAM	Institut de Radioastronomie Millimétrique
IUE	International Ultraviolet Explorer
LSR	Local Standard of Rest
MEM	Maximum Entropy Method
MHD	Magnetohydrodynamic
OVRO	Owens Valley Radio Observatory
RFI	Radio Frequency Interference

Continued on next page

Table A.1 – *Continued from previous page*

First entry	**Second entry**
S/N	signal-to-noise ratio
SOFIA	Stratospheric Observatory for Infrared Astronomy
SMA	Submillimeter Array
SZA	Sunyaev-Zel'dovich Array
SIS	superconductorinsulatorsuperconductor
UV	Ultraviolet
VLA	Karl G. Jansky Very Large Array
VLBA	Very Long Baseline Array
VLT	Very Large Telescope

B

Discrete Absorption Feature

The temperature equation outlined in Chapter 1 assumes that the wind is homogenous, but this may not be the case for Arcturus. During this study we analyzed STIS spectra of Arcturus from the online StarCAT catalog (Ayres, 2010). The Mg II h and k lines from data obtained in 2001 show a wind velocity $\sim 30 - 40$ km s^{-1}, which is similar to that adopted in the Drake models for this star Drake (1985). A narrow discrete absorption feature is found at -49 km s^{-1} in the broad blue-shifted wind absorption component of both lines as shown in Figure B.1. For this discrete feature we find a most probable turbulent velocity of 3.4 km s^{-1} and a Mg column density[1] of 1.4×10^{12} cm^{-2}. A Mg column density of 10^{15} cm^{-2} is required to produce the blueward absorption components in the h and k lines (McClintock *et al.*, 1978). Therefore, this discrete absorption feature accounts for $\sim 0.1\%$ of the total wind column density.

[1]Assuming all Mg to be Mg II

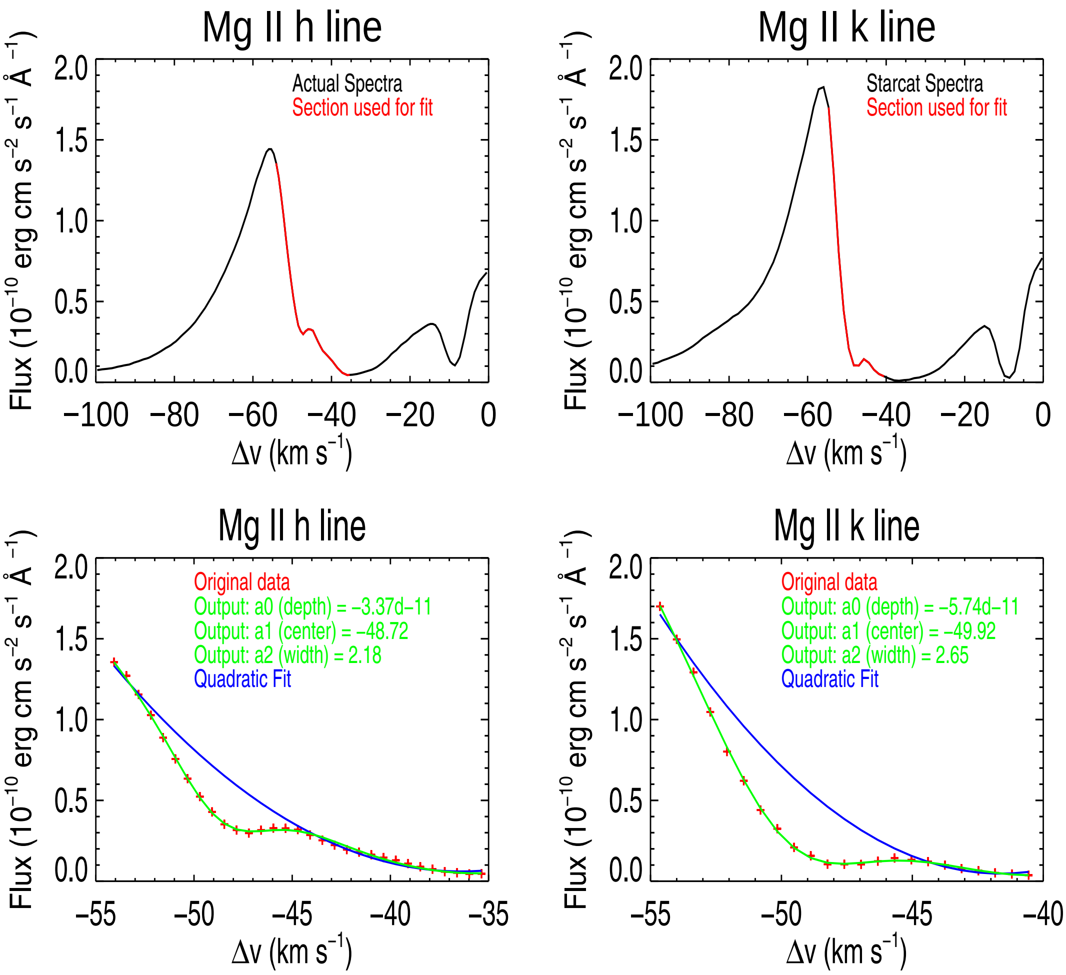

Figure B.1: Analysis on the absorption feature found in the Mg II *h* and *k* lines. A function composed of a linear combination of a Gaussian and a quadratic fitted the discrete absorption feature the best. The red data in the upper row shows the data that is used in this analysis.

C
Ambipolar Diffusion Heating

Considering a steady flow accelerating in an inertial frame, the equation of motion can be written as

$$\rho_n \boldsymbol{a}_n = \rho_n \boldsymbol{g} + \boldsymbol{f}_d \tag{C.1}$$

for the neutral species n, and

$$\rho_i \boldsymbol{a}_i = \rho_i \boldsymbol{g} - \boldsymbol{f}_d + \boldsymbol{f}_L \tag{C.2}$$

for the ion species, i. The flow acceleration is defined as $\boldsymbol{a} \equiv (\boldsymbol{v}.\nabla)\boldsymbol{v}$ and the gravitational acceleration is $\boldsymbol{g} \equiv \nabla(GM_\star/r)$. The volumetric drag force of the ions on the neutrals is defined as

$$\boldsymbol{f}_d = \gamma \rho_n \rho_i (\boldsymbol{v}_i - \boldsymbol{v}_n) \tag{C.3}$$

and $\boldsymbol{f}_L$ is the volumetric Lorentz force. The equation of motion for the combined ion-neutral fluid is found by addition of Equations C.1 and C.2

$$\rho \boldsymbol{a} = \rho \boldsymbol{g} + \boldsymbol{f}_L \tag{C.4}$$

where $\rho \equiv \rho_n + \rho_i$ is the mass density without the electrons and $\boldsymbol{a} \equiv (\rho_n \boldsymbol{a}_n + \rho_i \boldsymbol{a}_i)/\rho$ is the total acceleration.

The gravitational acceleration term can then be eliminated from Equations C.1 and C.2 to give

$$\boldsymbol{a}_n - \boldsymbol{a}_i = \left(\frac{1}{\rho_n} + \frac{1}{\rho_i}\right) \boldsymbol{f}_d - \frac{1}{\rho_i} \boldsymbol{f}_L. \tag{C.5}$$

Assuming then that the acceleration of the neutrals and ions are the same we get

$$\boldsymbol{f}_d = \left(\frac{\rho_n}{\rho_n + \rho_i}\right) \boldsymbol{f}_L. \tag{C.6}$$

This equation tells us that for a lightly ionized outflow the drag force is almost equal to the Lorentz force. We can now obtain an expression for the slip velocity, $\boldsymbol{w}$, by subbing this equation into Equation C.3

$$\boldsymbol{w} = \boldsymbol{v}_i - \boldsymbol{v}_n = \frac{\boldsymbol{f}_L}{\gamma \rho_i (\rho_n + \rho_n)}. \tag{C.7}$$

The slip velocity becomes large when the ion density becomes small, but does not become large when the neutral density becomes small because the large density of ions drag the few neutrals that are present along with the rest of the mostly ionized plasma. The heating rate per unit volume due to ambipolar diffusion heating is

$$\Gamma = \boldsymbol{f}_d . \boldsymbol{w} \tag{C.8}$$

and substitution of Equations C.6 and C.7 gives

$$\Gamma = \frac{\rho_n |\boldsymbol{f}_L|^2}{\gamma \rho_i (\rho_n + \rho_i)^2}, \tag{C.9}$$

and so for a completely ionized plasma, $\Gamma = 0$.

In order to calculate the ambipolar diffusion heating, we need to find a value for the ion-neutral momentum transfer coefficient, γ (in units $\mathrm{cm^3\,s^{-1}\,g^{-1}}$) which depends on the collisional coefficient rates, cross sections, slip speed, and gas composition. Shang *et al.* (2002) give the following expression

$$\gamma = \frac{2.13 \times 10^{14}}{1 - 0.714 x_e} \left(\left[3.23 + 41.0 T_4^{0.5} \times \left(1 + 1.338 \times 10^{-3} \frac{w_5^2}{T_4} \right)^{0.5} \right] x_{HI} + 0.243 \right) \tag{C.10}$$

where T_4 is the temperature in units of $10^4\,\mathrm{K}$, w_5 is the slip speed in units of $\mathrm{km\,s^{-1}}$. We have assumed no molecular hydrogen to be present and the fractional abundance of He, $x_{He} = 0.1$. Subbing Equation C.7 into Equation C.10 gives a quartic equation for γ, i.e.,

$$\gamma^4 - (2AE + 2ABx_{HI})\gamma^3 + (A^2E^2 + 2A^2BEx_{HI} + A^2B^2x_{HI}^2 - A^2C^2x_{HI}^2)\gamma^2 - GA^2C^2x_{HI}^2 = 0$$

where
$A = \frac{2.13\times10^{14}}{1-0.714x_e}$, $B = 3.23$, $C = 41.0T_4^{0.5}$, $D = \frac{1.338\times10^{-3}}{T_4}$, $E = 0.243$, $F = \frac{\boldsymbol{f}_L}{\rho_i(\rho_n+\rho_i)}$, and $G = \frac{DF^2}{1\times10^{10}}$. Finally the radial and azimuthal Lorentz forces and thus the corresponding volumetric ambipolar heating rates can be calculated by using the following expressions for the flow and gravitational accelerations:

$$\boldsymbol{a} = v\frac{dv}{dr}\boldsymbol{r} + \frac{v}{r}\frac{dv}{d\theta}\boldsymbol{\theta} + \frac{v}{r\sin\theta}\frac{dv}{d\phi}\boldsymbol{\phi} \tag{C.11}$$

and

$$\boldsymbol{g} = -\frac{GM_\star}{r^2}\boldsymbol{r} + \frac{1}{r}\frac{d}{d\theta}\left(\frac{GM_\star}{r}\right)\boldsymbol{\theta} + \frac{1}{r\sin\theta}\frac{d}{d\phi}\left(\frac{GM_\star}{r}\right)\boldsymbol{\phi}. \tag{C.12}$$

References

Asplund, M., Grevesse, N., Sauval, A.J. & Scott, P. (2009). The Chemical Composition of the Sun. *Annual Review of Astronomy & Astrophysics*, **47**, 481–522. (Cited on page 8.)

Ayres, T.R. (2010). StarCAT: A Catalog of Space Telescope Imaging Spectrograph Ultraviolet Echelle Spectra of Stars. *Astrophysical Journal Supplemental Series*, **187**, 149–171. (Cited on pages 11 and 18.)

Berger, T.E. & Title, A.M. (2001). On the Relation of G-Band Bright Points to the Photospheric Magnetic Field. *Astrophysical Journal*, **553**, 449–469. (Cited on page 14.)

Castor, J.I. (2004). *Radiation Hydrodynamics*. (Cited on page 8.)

Cranmer, S.R. (2012). Self-Consistent Models of the Solar Wind. *Space Science Reviews*, **172**, 145–156. (Cited on page 14.)

Cranmer, S.R. & Saar, S.H. (2011). Testing a Predictive Theoretical Model for the Mass Loss Rates of Cool Stars. *Astrophysical Journal*, **741**, 54. (Cited on page 13.)

Cranmer, S.R. & van Ballegooijen, A.A. (2005). On the Generation, Propagation, and Reflection of Alfvén Waves from the Solar Photosphere to the Distant Heliosphere. *Astrophysical Journal Supplemental Series*, **156**, 265–293. (Cited on page 14.)

Cranmer, S.R., van Ballegooijen, A.A. & Edgar, R.J. (2007). Self-consistent Coronal Heating and Solar Wind Acceleration from Anisotropic Magnetohydrodynamic Turbulence. *Astrophysical Journal Supplemental Series*, **171**, 520–551. (Cited on page 13.)

Dalgarno, A. & McCray, R.A. (1972). Heating and Ionization of HI Regions. *Annual Review of Astronomy & Astrophysics*, **10**, 375. (Cited on page 7.)

Decin, L., Vandenbussche, B., Waelkens, C., Decin, G., Eriksson, K., Gustafsson, B., Plez, B. & Sauval, A.J. (2003). ISO-SWS calibration and the accurate modelling of cool-star atmospheres. IV. G9 to M2 stars. *Astronomy & Astrophysics*, **400**, 709–727. (Cited on page 8.)

Drake, S.A. (1985). Modeling lines formed in the expanding chromospheres of red giants. In J.E. Beckman & L. Crivellari, eds., *Progress in stellar spectral line formation theory; Proceedings of the Advanced Research Workshop, Trieste, Italy, September 4-7, 1984 (A86-37976 17-90). Dordrecht, D. Reidel Publishing Co., 1985, p. 351-357.*, 351–357. (Cited on page 18.)

Falceta-Gonçalves, D., Vidotto, A.A. & Jatenco-Pereira, V. (2006). On the magnetic structure and wind parameter profiles of Alfvén wave driven winds in late-type supergiant stars. *Monthly Notices of the Royal Astronomical Society*, **368**, 1145–1150. (Cited on page 13.)

Goldreich, P. & Scoville, N. (1976). OH-IR stars. I - Physical properties of circumstellar envelopes. *Astrophysical Journal*, **205**, 144–154. (Cited on page 4.)

Hartmann, L. & MacGregor, K.B. (1980). Momentum and energy deposition in late-type stellar atmospheres and winds. *Astrophysical Journal*, **242**, 260–282. (Cited on page 13.)

Iroshnikov, P.S. (1964). Turbulence of a Conducting Fluid in a Strong Magnetic Field. *Soviet Astronomy*, **7**, 566. (Cited on page 14.)

Judge, P.G. (1986). Constraints on the outer atmospheric structure of late-type giant stars with IUE - Methods and application to Arcturus (Alpha Boo K2III). *Monthly Notices of the Royal Astronomical Society*, **221**, 119–153. (Cited on page 7.)

Lehe, R., Parrish, I.J. & Quataert, E. (2009). The Heating of Test Particles in Numerical Simulations of Alfvénic Turbulence. *Astrophysical Journal*, **707**, 404–419. (Cited on page 13.)

Lighthill, M.J. (1952). On Sound Generated Aerodynamically. I. General Theory. *Royal Society of London Proceedings Series A*, **211**, 564–587. (Cited on page 13.)

Mathisen, R. (1984). Photo cross-sections for stellar atmosphere calculations – compilation of references and data. Inst. Theor. Astrophys. Univ. Oslo, publ. Series No. 1. (Cited on page 11.)

Matthaeus, W.H., Zank, G.P., Oughton, S., Mullan, D.J. & Dmitruk, P. (1999). Coronal Heating by Magnetohydrodynamic Turbulence Driven by Reflected Low-Frequency Waves. *Astrophysical Journal Letters*, **523**, L93–L96. (Cited on page 14.)

McClintock, W., Moos, H.W., Henry, R.C., Linsky, J.L. & Barker, E.S. (1978). Ultraviolet observations of cool stars. VI - L alpha and MG II emission line profiles (and a search for flux variability) in Arcturus. *Astrophysical Journal Supplemental Series*, **37**, 223–233. (Cited on page 18.)

O'Gorman, E. & Harper, G.M. (2011). What is Heating Arcturus' Wind? In C. Johns-Krull, M.K. Browning & A.A. West, eds., *16th Cambridge Workshop on Cool Stars, Stellar Systems, and the Sun*, vol. 448 of *Astronomical Society of the Pacific Conference Series*, 691. (Cited on page 1.)

Ramírez, I. & Allende Prieto, C. (2011). Fundamental Parameters and Chemical Composition of Arcturus. *Astrophysical Journal*, **743**, 135. (Cited on page 8.)

Rodgers, B. & Glassgold, A.E. (1991). The temperature of the circumstellar envelope of Alpha Orionis. *Astrophysical Journal*, **382**, 606–616. (Cited on page 4.)

Schrijver, C.J. & Harvey, K.L. (1989). The distribution of solar magnetic fluxes and the nonlinearity of stellar flux-flux relations. *Astrophysical Journal*, **343**, 481–488. (Cited on page 14.)

Sennhauser, C. & Berdyugina, S.V. (2011). First detection of a weak magnetic field on the giant Arcturus: remnants of a solar dynamo? *Astronomy & Astrophysics*, **529**, A100. (Cited on pages 12 and 14.)

Shang, H., Glassgold, A.E., Shu, F.H. & Lizano, S. (2002). Heating and Ionization of X-Winds. *Astrophysical Journal*, **564**, 853–876. (Cited on pages 12 and 22.)

Spitzer, L. (1978). *Physical processes in the interstellar medium*. New York Wiley-Interscience, 1978. 333 p. (Cited on pages 6, 7 and 12.)

Stein, R.F. (1967). Generation of Acoustic and Gravity Waves by Turbulence in an Isothermal Stratified Atmosphere. *Solar Physics*, **2**, 385–432. (Cited on page 13.)